Vahid Nazari[1]
Department of Mechanical and Materials Engineering,
Queen's University,
Kingston, ON K7L 3N6, Canada
e-mail: v.nazari@queensu.ca

Leila Notash
Department of Mechanical and Materials Engineering,
Queen's University,
Kingston, ON K7L 3N6, Canada
e-mail: leila.notash@queensu.ca

Motion Analysis of Manipulators With Uncertainty in Kinematic Parameters

In this article, a novel method for characterizing the exact solution for interval linear systems is presented. In the proposed method, the entries of the interval coefficient matrix and interval right-hand side vector are formulated as linear functions of two or three parameters. The parameter groups for two- and three-parameter cases are identified. The exact solution is characterized using the solution sets corresponding to the parameter groups. The parametric method is then employed in the motion analysis of manipulators considering the uncertainty in kinematic parameters. Example manipulators are used to show the implementation of the method and the effect of uncertainty in the motion performance. [DOI: 10.1115/1.4031657]

1 Introduction

Robot manipulators have moved from reachable environments of laboratories and factories into the hazardous or remote environments in order to reduce the time, cost, and risk involved in preparing humans to endure these conditions. Manipulators are typical of real systems that are intrinsically subject to uncertainties. The nominal relationship between the end effector pose and the joint displacements is known but this relationship is not necessarily accurate due to uncertainties in kinematic parameters [1]. All these uncertainties are accommodated as bounded intervals so that the real value of a given parameter lies within the interval. Interval analysis is a numerical method of representing uncertainty in values by replacing a number with a finite range of values. The significance of the interval analysis is that it is able to solve problems that cannot be efficiently solved using traditional numerical approximation methods. Interval analysis keeps track of all error types simultaneously because an interval arithmetic operation produces a closed interval within which the true real-valued result is guaranteed to lie [2].

Interval analysis was first introduced by Moore in early 1960 s to analyze and control numerical errors in computers [3]. Now, interval analysis is widely used to deal with uncertain data in areas such as electrical engineering, structure engineering, control theory, quality control, dynamical and chaotic systems, signal processing, computer graphics, and robotics. One of the first applications of the interval analysis in robotics was for solving the inverse displacement problems for serial robots using interval version of the Newton method [4]. This numerical technique employed the interval evaluation of the inverse of the Jacobian matrix involved in the Taylor remainder and was only applicable to systems with nonsingular Jacobian matrix. The forward displacement of a Gough–Stewart platform was numerically studied in Ref. [5]. The efficiency of nonlinear interval arithmetic was improved by filleting technique. Interval arithmetic with bisection technique was used in Ref. [6] to check the singular configurations of a Gough–Stewart platform. In Ref. [7], global optimization including interval analysis was proposed to determine the best configuration of a redundant serial manipulator for a peg-in-hole task. The reliability estimation method was applied in Ref. [8] to the systems modeled by fault trees with input uncertainty represented by interval. Interval Newton method was used in Ref. [9] to calibrate the kinematic parameters in parallel robots. The interval method calculated the ranges for parameters to satisfy the calibration equations.

Several methods are known for calculating the lower and upper bounds for each component of the solution set in the interval linear systems. One of the first contributions on determining the bounds of the solution set was given in Ref. [10]. More general algorithms to determine the bounds of the solution in the interval linear system were presented in Refs. [11–13].

Mathematically, the exact solution of the interval linear system $[\mathbf{A}]\mathbf{x} = [\mathbf{b}]$ is defined as the region that includes all vectors described as $\mathbf{x} = \mathbf{A}^{-1}\mathbf{b}$ for all $\mathbf{A} \in [\mathbf{A}]$ and $\mathbf{b} \in [\mathbf{b}]$ as long as $\mathbf{A} \in [\mathbf{A}]$ is nonsingular. The exact solution of the interval linear system is essential in robot applications such as workspace determination, motion analysis, trajectory tracking, and design process, where the manipulator has uncertainty in its parameters. For example, when a manipulator with uncertain parameters follows a trajectory, all components of the joint velocity vector should be within the exact solution of the joint velocity. The exact solution was determined in Ref. [14] as the union of finitely many convex polytopes whose vertices were denoted by matrices with entries equal to the lower or upper bounds of the interval coefficient matrix. The shape of the solution set, in general, is nonconvex polyhedron. The exact solution of the interval linear systems is generally complicated and cannot be described in the form of interval. Therefore, calculation of this solution is computationally expensive. Accordingly, the researchers are drawn to find the fastest methods to enclose the exact solution. Most of these methods are not necessarily optimal. From the optimality point of view, an interval solution which is much more convenient to use is the smallest box containing the exact solution which is called the interval hull of the solution set. A procedure for computing the interval hull was given in Ref. [15].

Linear dependences in matrix entries and the right-hand side vector components of the interval linear systems were investigated by several researchers. The first work on parametric interval systems was given in Ref. [16] where the bounds of solution set of the parameterized interval linear system with special coefficient matrices, such as symmetric or skew-symmetric matrices, were calculated. The general solution of the parameterized interval linear system was first investigated in Ref. [17]. The boundary of the solution set of the parametric linear system was provided in Ref. [18] where the entries of the coefficient matrix and the right-hand side vector were functions of parameters varying within interval bounds. The solution was only for one group of parametric linear system which was smaller than the solution of the corresponding interval linear system.

The objective of this article is to investigate the effect of uncertainty in kinematic parameters on the motion performance of manipulators. For the known range of uncertainties in kinematic parameters and the given end effector twist, the interval of the joint velocity vector is calculated. This article is laid out in the

[1]Corresponding author.

Manuscript received March 16, 2015; final manuscript received September 6, 2015; published online November 24, 2015. Assoc. Editor: Raffaele Di Gregorio.

following manner. The basic principles of interval analysis in modeling uncertainty in the Denavit–Hartenberg (D–H) parameters of manipulators are presented in Sec. 2. In Sec. 3, the parametric linear systems, its regularity, and application to the Jacobian matrix of manipulators are introduced. A novel approach for characterizing the exact solution in the interval linear system is presented in Sec. 4. In Sec. 5, the interval analysis is applied to calculate the velocity of the joints of planar serial and parallel manipulators with uncertainty in kinematic parameters taking into account the joint velocity limits, and the simulation results are reported. Finally, conclusions are given in Sec. 6.

2 Uncertainty in Robot Manipulators

Dealing with uncertainty in robot manipulators is one of the challenging problems, which has been drawing considerable attentions among researchers. Analysis of a real robot such as failure and workspace analysis should be performed in the presence of uncertainty in the model of the manipulator and measurements of kinematic parameters. The sources of uncertainty are the manufacturing tolerances of the mechanical parts, measurement error, control error, and round-off error. These types of uncertainty can be accommodated as bounded variations in kinematic parameters.

All nominal calculations are based on the perfect knowledge of kinematic parameters of the manipulators. In the prototyped manipulators, however, there are bounded errors on the link lengths and joint measurements. Because of the errors, which are due to inherently inaccurate nature of the measurements, the kinematic and static force equations remain valid although their equations form interval linear systems. Consequently, there is no finite number of solutions to the interval linear systems but a bound for the solution is provided.

2.1 Interval Analysis. Interval analysis is a numerical method of representing uncertainty in values by replacing a number with a finite range of values. In this paper, all interval vectors/matrices will be denoted within square brackets to differentiate them from the point/real vectors/matrices. An interval denoted by $[\mathrm{X}] = [\underline{\mathrm{X}}, \overline{\mathrm{X}}]$ is the set of real numbers X verifying $\underline{\mathrm{X}} \le \mathrm{X} \le \overline{\mathrm{X}}$, where $\underline{\mathrm{X}}$ and $\overline{\mathrm{X}}$ are the lower and upper bounds of the interval, respectively. The interval is also represented by the midpoint, $\mathrm{X_c}$, and radius, $\Delta\mathrm{X}$, as $[\mathrm{X}] = [\mathrm{X_c} - \Delta\mathrm{X}, \mathrm{X_c} + \Delta\mathrm{X}]$ or $[\mathrm{X}] = \mathrm{X_c} + \Delta\mathrm{X}\,[-1, 1]$. A real number is a special case of an interval in which $\underline{\mathrm{X}} = \overline{\mathrm{X}}$. The width of the interval [X] is defined as $(\mathrm{X}) = \overline{\mathrm{X}} - \underline{\mathrm{X}}$. The absolute value of [X], denoted by $|\mathrm{X}|$, is the maximum of the absolute values of its bounds, $|\mathrm{X}| = \max\{|\overline{\mathrm{X}}|, |\underline{\mathrm{X}}|\}$. The midpoint of [X] is given by $m(\mathrm{X}) = (1/2)(\overline{\mathrm{X}} + \underline{\mathrm{X}})$.

An interval vector is a set of intervals and its width is defined as the largest width of its interval members, while its center is defined as the midpoint of the interval members. A matrix whose entries are interval is called an interval matrix. The midpoint of an interval matrix [**A**] is the real matrix whose entries are the midpoints of the entries of [**A**]. The norm of the interval matrix [**A**], denoted by **A**, is defined as $\max_i \sum_j |a_{ij}|$, which is an interval extension of the maximum row sum norm for real matrices [19].

2.2 Jacobian Matrix of Serial Manipulators With Uncertainty in D–H Parameters. In serial manipulators, the error of the end effector pose (position and orientation) within its workspace is characterized by modeling uncertainties of kinematic parameters. For the analysis presented in this article, a coordinate frame is attached to each joint and the D–H convention developed in Ref. [20] is applied (modified D–H parameters represented in Ref. [21] for modeling two consecutive parallel joint axes).

There exists a finite change between the two consecutive coordinate frames $j-1$ and j due to small errors in kinematic parameters of these coordinate frames. The errors between two consecutive coordinate frames from the base to the end effector of a serial manipulator are accumulated and the relationship between the errors of D–H parameters in all links and the error of the end effector pose is characterized using

$$\mathbf{A}_{0,j} = \mathbf{A}_{0,1}\mathbf{A}_{1,2}\ldots\mathbf{A}_{j-1,j} \tag{1}$$

where $\mathbf{A}_{j-1,j}$ is the homogeneous transformation matrix between the two consecutive coordinate frames $j-1$ and j. The interval of each D–H parameter in joint j, e.g., twist angle $[\alpha_j]$, is defined as a bounded set of real numbers, where the nominal value of each parameter is the midpoint of the interval and the deviation from the nominal value is the radius of uncertainty. For example, the lower and upper bounds of the interval $[\alpha_j]$ are defined as

$$[\underline{\alpha}_j, \overline{\alpha}_j] = \alpha_{cj} + [\delta\alpha_j], \quad \delta\alpha_j > 0 \tag{2}$$

where α_{cj} is the midpoint, $\delta\alpha_j$ is the radius of the uncertainty in parameter, and $[\delta\alpha_j] = [\underline{\delta\alpha}_j, \overline{\delta\alpha}_j]$ is the interval which indicates the maximum deviation from the nominal value of parameter α_{cj} and $\overline{\delta\alpha}_j = -\underline{\delta\alpha}_j = \delta\alpha_j$. The actual deviation of each parameter from its nominal value is a real number which lies in the interval. The uncertainty of other parameters is defined in the same way and includes $[\delta a_j] = [\underline{\delta a}_j, \overline{\delta a}_j]$, $[\delta\theta_j] = [\underline{\delta\theta}_j, \overline{\delta\theta}_j]$, and $[\delta d_j] = [\underline{\delta d}_j, \overline{\delta d}_j]$.

Considering a serial manipulator with the task space dimension of m and l active joints, the $l \times 1$ joint velocity vector, $\dot{\mathbf{q}} = [\,\dot{q}_1 \quad \dot{q}_2 \quad \ldots \quad \dot{q}_l\,]^{\mathrm{T}}$, and the $m \times 1$ end effector twist, **V**, are related by the $m \times l$ Jacobian matrix **J** as

$$\mathbf{V} = \begin{bmatrix} \mathbf{v} \\ \boldsymbol{\omega} \end{bmatrix} = \mathbf{J}\dot{\mathbf{q}} = [\,\mathbf{J}_1 \quad \mathbf{J}_2 \quad \ldots \quad \mathbf{J}_l\,]\,\dot{\mathbf{q}} = \sum_{j=1}^{l} \mathbf{J}_j \dot{q}_j \tag{3}$$

where **v** is the translational velocity vector of the operation point of the end effector and $\boldsymbol{\omega}$ is the angular velocity vector of the end effector. With interval parameters, the interval Jacobian matrix of manipulator $[\mathbf{J}] = ([\mathbf{J}_1] \quad [\mathbf{J}_2] \quad \ldots \quad [\mathbf{J}_l])$ relates the interval joint velocity vector to the interval end effector twist [**V**]

$$[\mathbf{V}] = [\mathbf{J}][\dot{\mathbf{q}}] = \sum_{j=1}^{l} [\mathbf{J}_j][\dot{q}_j] \tag{4}$$

3 Parameterized Linear Systems

The relation between the joint velocity vector and the end effector twist of a serial manipulator is given by the system of linear equations $[\mathbf{J}]\dot{\mathbf{q}} = [\mathbf{V}]$ or

$$\sum_{j=1}^{l} [J_{kj}]\dot{q}_j = [\mathrm{V}_k] \text{ and } k = 1, 2, \ldots, m \tag{5}$$

Before calculating the interval enclosures of the joint velocities, the regularity of the interval Jacobian matrix is checked. An interval matrix [**J**] is called regular if each $\mathbf{J} \in [\mathbf{J}]$ is nonsingular, otherwise it is said to be singular, i.e., if [**J**] contains a singular matrix. A sufficient condition for regularity of an interval square Jacobian matrix is when the following inequality holds [22]:

$$\rho(|\mathbf{J}_{\mathrm{c}}^{-1}|\Delta\mathbf{J}) < 1 \tag{6}$$

where $[\underline{\mathbf{J}}, \overline{\mathbf{J}}] = [\mathbf{J}_{\mathrm{c}} - \Delta\mathbf{J}, \mathbf{J}_{\mathrm{c}} + \Delta\mathbf{J}]$, $\mathbf{J}_c$ is the midpoint of the interval Jacobian matrix, $\Delta\mathbf{J}$ is the radius of the interval matrix; and $\rho(|\mathbf{J}_{\mathrm{c}}^{-1}|\Delta\mathbf{J})$ is the spectral radius of square matrix $|\mathbf{J}_{\mathrm{c}}^{-1}|\Delta\mathbf{J}$, which is defined as the maximum eigenvalue of the matrix and the entries of matrix $|\mathbf{J}_{\mathrm{c}}^{-1}|$ are the absolute values of the corresponding entries of matrix $\mathbf{J}_{\mathrm{c}}^{-1}$.

In real applications, the calculated values of the entries of [**J**]and [**V**], denoted by J_{jk} and V_j, are based on the measurement and include uncertainties. For a given interval end effector twist and interval Jacobian matrix, the problem is to find the solution set, i.e., the set of all vectors $\dot{\mathbf{q}} = [\dot{q}_1 \quad \dot{q}_2 \quad \ldots \quad \dot{q}_l]^{\mathrm{T}}$ for which $\sum_{j=1}^{l} J_{kj}\dot{q}_j = \mathrm{V}_k$ for some $J_{kj} \in [J_{kj}]$ and $\mathrm{V}_k \in [\mathrm{V}_k], k = 1, 2, \ldots, m, j = 1, 2, \ldots, l$. In other words,

$$\dot{\mathbf{q}} : \mathbf{J}\dot{\mathbf{q}} = \mathbf{V} \quad \text{for some } \mathbf{J} \in [\mathbf{J}], \quad \mathbf{V} \in [\mathbf{V}] \tag{7}$$

There exist several methods for calculating the lower and upper bounds for each component of the solution set in the interval linear systems. The most applicable interval methods are interval Gaussian elimination method, linear Krawczyk method, interval Gauss–Seidel method, and interval hull method. These methods provide an interval vector containing the solution to the interval linear system but the boundary of the exact solution is not identified by these methods. In Sec. 4, a novel method for calculating the exact solution for the interval linear system will be presented.

3.1 Parametric System of Interval Linear Equations. A set of parametric interval equations is a linear system $[\mathbf{J}([\mathbf{p}])]\dot{\mathbf{q}} = [\mathbf{V}([\mathbf{p}])]$ in terms of $\dot{\mathbf{q}}$ in which the entries of the coefficient matrix $[\mathbf{J}] \in \mathbb{R}^{m\times l}$ and the right-hand side vector $[\mathbf{V}] \in \mathbb{R}^{m}$ depend on K number of interval parameters $[\mathbf{p}] = ([p_1], [p_2], \ldots, [p_K])$. To differentiate the interval parameters from the real parameters, square brackets are used which indicate that the parameters are interval. The exact values of these parameters are unknown but bounded within given intervals. For manipulators, the entries of $[\mathbf{J}]$ and $[\mathbf{V}]$ can be parameterized as linear functions of K interval parameters $[\mathbf{p}]$.

$$\begin{aligned}[J_{jk}]([\mathbf{p}]) &= J_{jk,0} + \sum_{\mu=1}^{K} J_{jk,\mu}[p_\mu] \\ [V_j]([\mathbf{p}]) &= V_{j,0} + \sum_{\mu=1}^{K} V_{j,\mu}[p_\mu]\end{aligned} \tag{8}$$

where $J_{jk,\mu}, V_{j,\mu} \in \mathbb{R}; \mu = 1, \ldots, K;\ j = 1, \ldots, m; k = 1, \ldots, l;\ m$ is the task space dimension and l is the number of active joints in the manipulator. The entries of the coefficient matrix and the right-hand side vector can be linear or nonlinear functions of the interval parameters $[\mathbf{p}]$. In this paper, a linear model is used.

3.2 Regularity of Parametric Interval Matrices. In order to characterize the solution set for the parameterized linear system with entries defined in Eq. (8), the regularity of the parametric square Jacobian matrix $[\mathbf{J}([\mathbf{p}])]$ of the manipulators should be checked. The sufficient condition for the regularity of parametric square interval matrices with entries as linear functions of parameters was studied in Ref. [23]. If nonparametric square interval matrix $[\mathbf{J}]$ is regular, then $[\mathbf{J}([\mathbf{p}])]$ will be regular for $[\mathbf{p}]$. For a preconditioned parametric interval matrix, if the following inequality is satisfied:

$$\rho\left(\left|\mathbf{I} - \mathbf{B}\mathbf{J}(\mathbf{p}_c)\right| + \sum_{\mu=1}^{K} \Delta p_\mu \left|\mathbf{B}\mathbf{J}_\mu\right|\right) < 1 \tag{9}$$

then $[\mathbf{J}([\mathbf{p}])]$ is regular. The proof is detailed in Ref. [24]. In inequality (9), $\rho(.)$ is the spectral radius of the real matrix $(|\mathbf{I} - \mathbf{B}\mathbf{J}(\mathbf{p}_c)| + \sum_{\mu=1}^{K} \Delta p_\mu |\mathbf{B}\mathbf{J}_\mu|)$, $\mathbf{B}$ is the preconditioner, $\mathbf{p}_c$ is the vector of the midpoint of the interval parameters $\mathbf{p}_c = (p_{1c}, p_{2c}, \ldots, p_{Kc})$, $\mathbf{J}(\mathbf{p}_c)$ is the real matrix whose entries are the midpoints of the entries of $[\mathbf{J}([\mathbf{p}])]$, Δp_μ is the radius of the interval parameter $[p_\mu]$, and $\mathbf{J}_\mu \in \mathbb{R}^{m\times l}$ is the real matrix with entries $J_{jk,\mu}$ defined in Eq. (8). The most commonly used matrix $\mathbf{B}$ is the numerically computed midpoint inverse of $[\mathbf{J}([\mathbf{p}])]$. If the real matrix $\mathbf{J}(\mathbf{p}_c)$ is square and nonsingular and $\mathbf{B}$ is the inverse of $\mathbf{J}(\mathbf{p}_c)$, then $|\mathbf{I} - \mathbf{B}\mathbf{J}(\mathbf{p}_c)| = |\mathbf{I} - \mathbf{J}^{-1}(\mathbf{p}_c)\mathbf{J}(\mathbf{p}_c)| = 0$ and Eq. (9) is simplified as

$$\rho\left(\sum_{\mu=1}^{K} \Delta p_\mu \left|\mathbf{J}(\mathbf{p}_c)^{-1}\mathbf{J}_\mu\right|\right) < 1 \tag{10}$$

4 Parametric Groups and Exact Solution

In this section, the exact solution of the parameterized interval linear system obtained in Sec. 3 is formulated. The parameter assignment of the entries of the interval Jacobian matrix $[\mathbf{J}]$ and the interval twist vector $[\mathbf{V}]$ of manipulators is performed by formulating the interval entries of $[\mathbf{J}]$ and $[\mathbf{V}]$ as functions of interval parameters $[p_\mu]$. Each interval entry is a function of one parameter among parameters $[p_\mu], \mu = 1, \ldots, K$.

The number of parameter groups in each interval system depends on the number of interval entries of $[\mathbf{J}([\mathbf{p}])]$ and $[\mathbf{V}([\mathbf{p}])]$, η, and the number of interval parameters used, K. The solution sets of all parameter assignments of the interval system are checked and the parameter assignments for the entries of $[\mathbf{J}]$ and $[\mathbf{V}]$ which result in the same solution set are categorized as one-parameter group.

If $[\mathbf{J}([\mathbf{p}])]$ is an $n \times n$ square matrix and nonsingular for every $p_\mu \in [\underline{p_\mu}, \overline{p_\mu}], \mu = 1, \ldots, K$, $[\mathbf{J}^{-1}([\mathbf{p}])]$ exists and $[\dot{\mathbf{q}}([\mathbf{p}])] = [\mathbf{J}^{-1}([\mathbf{p}])][\mathbf{V}([\mathbf{p}])]$ is a function of K interval parameters which is continuous [18]. When the entries of $[\mathbf{J}([\mathbf{p}])]$ and $[\mathbf{V}([\mathbf{p}])]$, i.e., entries $[J_{jk}]$ and $[V_j]$, are formulated as linear functions of the interval parameter $[p_\mu]$, $1 \le \mu \le K$, then,

$$\begin{aligned}[J_{jk}([p_\mu])] &= J_{jk,0} + J_{jk,1}[p_\mu] \\ [V_j([p_\mu])] &= V_{j,0} + V_{j,1}[p_\mu]\end{aligned} \tag{11}$$

where $j, k = 1, 2, \ldots, n$. In Eq. (11), the interval parameter $[p_\mu]$ is dimensionless and the corresponding coefficients, e.g., $J_{jk,0}$ and $J_{jk,1}$, have the units of the pertinent entry of $[\mathbf{J}]$ or $[\mathbf{V}]$, e.g., entry J_{jk} of $[\mathbf{J}]$. The lower and upper bounds of any interval entry $[J_{jk}] = [\underline{J_{jk}}, \overline{J_{jk}}]$ are related to those of interval parameter $p_\mu \in [\underline{p_\mu}, \overline{p_\mu}], \underline{p_\mu} \ne \overline{p_\mu}$ through a system of linear equations

$$\begin{cases} \overline{J_{jk}} = J_{jk,0}\overline{p_\mu} + J_{jk,1} \\ \underline{J_{jk}} = J_{jk,0}\underline{p_\mu} + J_{jk,1} \end{cases} \Rightarrow \begin{bmatrix} \overline{p_\mu} & 1 \\ \underline{p_\mu} & 1 \end{bmatrix} \begin{bmatrix} J_{jk,0} \\ J_{jk,1} \end{bmatrix} = \begin{bmatrix} \overline{J_{jk}} \\ \underline{J_{jk}} \end{bmatrix} \tag{12}$$

The coefficients $J_{jk,0}$ and $J_{jk,1}$ are calculated by taking the inverse of the matrix in Eq. (12) as

$$\begin{bmatrix} J_{jk,0} \\ J_{jk,1} \end{bmatrix} = \begin{bmatrix} \overline{p_\mu} & 1 \\ \underline{p_\mu} & 1 \end{bmatrix}^{-1} \begin{bmatrix} \overline{J_{jk}} \\ \underline{J_{jk}} \end{bmatrix} \tag{13}$$

It should be noted that the entry nominated for the interval parameter must be interval. Otherwise, the matrix in Eq. (12) would be singular and the interval entry $[J_{jk}]$ cannot be formulated in terms of parameter $[p_\mu]$. The same procedure is performed to formulate the entry $[V_j]$ as a function of $[p_\mu]$. If the interval Jacobian matrix $[\mathbf{J}]$ and the end effector twist $[\mathbf{V}]$ have entries with real value, the corresponding coefficients $J_{jk,1}$ and $V_{j,1}$ in Eq. (11) are zero and these entries will not be functions of $[p_\mu]$. In Secs. 4.1, 4.2, and 4.3, the formulations of solutions sets for one, two, and three parameters are presented with an example serial manipulator.

4.1 One-Parameter Solution Set. In the one-parameter case, i.e., $K = 1$, the interval entries of the coefficient matrix and right-hand side vector are parameterized as linear functions of $[p_1]$. To appreciate the procedure, a 2DOF (degrees-of-freedom) planar serial manipulator depicted in Fig. 1 is considered. The manipulator includes two revolute joints and two links. Joint displacements

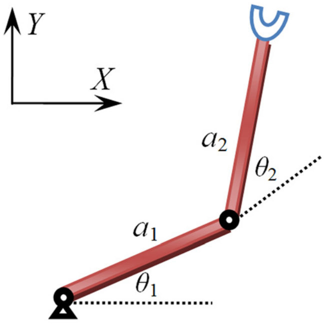

Fig. 1 Two degrees-of-freedom planar serial manipulator

θ_1 and θ_2 have uncertainties and other D–H parameters, i.e., $a_1, a_2, d_1, d_2, \alpha_1, \alpha_2, \beta_1$, and β_2, have no uncertainty.

For joint variables $\theta_1 = (\pi/6)$ rad and $\theta_2 = (\pi/4)$ rad, link lengths $a_1 = a_2 = 0.5$ m, radius of uncertainty $(\pi/180)$ rad in the joint displacements with the end effector twist $\mathbf{V} = [v_x v_y]^{\mathrm{T}} = [11]^{\mathrm{T}}$ (m/s), the interval system is formulated as

$$\begin{pmatrix} [-0.745, -0.720] & [-0.487, -0.478] \\ [0.541, 0.584] & [0.112, 0.146] \end{pmatrix} \begin{pmatrix} \dot{\theta}_1 \\ \dot{\theta}_2 \end{pmatrix} = \begin{pmatrix} [1, 1] \\ [1, 1] \end{pmatrix} \tag{14}$$

If the Jacobian matrix and the end effector twist are functions of one parameter $[p_1]$, i.e., $K = 1$, the parametric linear system will be defined as

$$\begin{pmatrix} [J_{11}([p_1])] & [J_{12}([p_1])] \\ [J_{21}([p_1])] & [J_{22}([p_1])] \end{pmatrix} \begin{bmatrix} \dot{\theta}_1 \\ \dot{\theta}_2 \end{bmatrix} = \begin{pmatrix} v_x \\ v_y \end{pmatrix} \tag{15}$$

The parameter solution set is derived using the inverse of $[\mathbf{J}([p_1])]$ as

$$\left[\dot{\boldsymbol{\theta}}([p_1])\right] = \begin{pmatrix} [\dot{\theta}_1([p_1])] \\ [\dot{\theta}_2([p_1])] \end{pmatrix} = \begin{pmatrix} [J_{11}([p_1])] & [J_{12}([p_1])] \\ [J_{21}([p_1])] & [J_{22}([p_1])] \end{pmatrix}^{-1} \begin{pmatrix} v_x \\ v_y \end{pmatrix} \tag{16}$$

Entry J_{11} is selected as $J_{11} = p_1 \in [-0.745, -0.721]$, with $J_{11,0} = 0$ and $J_{11,1} = 1$. Applying Eq. (13), the parameterized interval system is formulated as

$$\begin{pmatrix} [p_1] & 0.374[p_1] - 0.209 \\ 1.757[p_1] + 1.850 & 1.396[p_1] + 1.152 \end{pmatrix} \begin{bmatrix} \dot{\theta}_1 \\ \dot{\theta}_2 \end{bmatrix} = \begin{pmatrix} [1, 1] \\ [1, 1] \end{pmatrix} \tag{17}$$

The parametric Jacobian matrix $[\mathbf{J}([p_1])]$ for $p_1 \in [-0.745 - 0.721]$ is regular as the spectral radius of $(|\mathbf{I} - \mathbf{BJ}(p_{1c})| + \Delta p_1 |\mathbf{BJ}_1|) = 0.1602 < 1$. $\mathbf{J}(p_{1c})$ is the midpoint of the interval matrix in Eq. (17) and $\mathbf{J}_1$ is the matrix whose entries are coefficients of $[p_1]$ in the Jacobian matrix of Eq. (17). Therefore, taking the inverse of $[\mathbf{J}([p_1])]$ leads to the parameter solution set

$$\left[\dot{\boldsymbol{\theta}}([p_1])\right] = \begin{pmatrix} \left[\dot{\theta}_1([p_1])\right] \\ \left[\dot{\theta}_2([p_1])\right] \end{pmatrix} = \begin{pmatrix} \dfrac{1.030[p_1] + 1.360}{0.749[p_1]^2 + 0.835[p_1] + 0.389} \\ \dfrac{-0.760[p_1] - 1.850}{0.749[p_1]^2 + 0.835[p_1] + 0.389} \end{pmatrix} \tag{18}$$

The one-parameter solution set is a line and is illustrated in Fig. 2(*a*). The outer enclosure formed by dashed lines represents the exact solution (exact solution is formulated in Sec. 4.2). The one-parameter solution set is inside the exact solution, and hence, is not sufficient to characterize the exact solution of the interval linear system. It is worth noting that, no matter which entry of

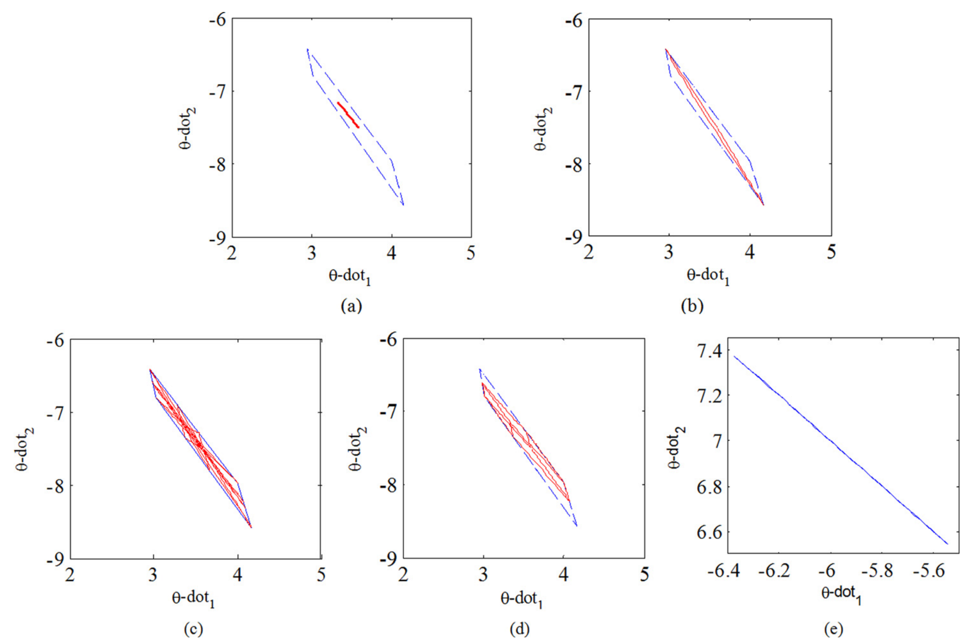

Fig. 2 (*a*) One-parameter solution set, solid line, and the exact solution, dashed lines, (*b*) one of two-parameter solution sets represented with solid lines, (*c*) all two-parameter solution sets, dashed lines, (*d*) one of three-parameter solution sets, solid lines, and (*e*) two-parameter solution set in Eq. (20) when $\theta_1 = (\pi/6)$ (rad), $\theta_2 = (\pi/4)$ (rad), and the radius of uncertainty is $(\pi/180)$ (rad)

$[\mathbf{J}([p_1])]$ is set to be an interval parameter, the same solution line will be obtained, i.e., there is only one parameter group.

4.2 Two-Parameter Solution Set. In the two-parameter case, i.e., $K=2$, the interval entries of the coefficient matrix and right-hand side vector are linearly formulated in terms of $[p_1]$ or $[p_2]$. It is worth mentioning that the following parameter assignments of the Jacobian matrix of the 2DOF manipulator of Sec. 4.1 $\begin{pmatrix} [p_1] & [p_2] \\ [J_{21}([p_2])] & [J_{22}([p_1])] \end{pmatrix}$, $\begin{pmatrix} [p_1] & [J_{12}([p_2])] \\ [p_2] & [J_{22}([p_1])] \end{pmatrix}$, $\begin{pmatrix} [J_{11}([p_1])] & [J_{12}([p_2])] \\ [p_2] & [p_1] \end{pmatrix}$, and $\begin{pmatrix} [J_{11}([p_1])] & [p_2] \\ [J_{21}([p_2])] & [p_1] \end{pmatrix}$ with the same end effector twist $[v_x\ v_y]^{\mathrm{T}}$ lead to the same parameter solution set. These four parameterized Jacobian matrices with diagonal entries as functions of $[p_1]$, no matter which one of the parameters is the interval parameter $[p_1]$, and the other entries as functions of $[p_2]$ are categorized into one-parameter group.

For a spatial manipulator, to form $[\mathbf{J}]\,\dot{\mathbf{q}}=[\mathbf{V}]$, with a total of $\eta \le ml+m$ interval entries in $[\mathbf{J}]$ and $[\mathbf{V}]$, and two interval parameters, $K=2$, there exist $(1/2)\sum_{j=1}^{\eta-1}(\eta/j) = (1/2)\sum_{j=1}^{\eta-1}[\eta!/((\eta-j)!j!)]$ different parameter groups. These calculations are also valid when entries of either Jacobian matrix $[\mathbf{J}([\mathbf{p}])]$ or end effector twist $[\mathbf{V}([\mathbf{p}])]$ are nonlinear functions of parameters $[p_1]$ and $[p_2]$. Parameter K represents the number of the interval parameters used to form the parameterized matrix $[\mathbf{J}([\mathbf{p}])]$ and vector $[\mathbf{V}([\mathbf{p}])]$. For example, in an interval system $[\mathbf{J}]\,\dot{\mathbf{q}}=[\mathbf{V}]$ where $[\mathbf{J}]\in\mathbb{R}^{2\times2}$ and $[\mathbf{V}]\in\mathbb{R}^2$, if all entries of the Jacobian matrix and twist are interval, $\eta=6$, and two interval parameters, $K=2$, are used to parameterize the interval system, there will be $(1/2)\sum_{i=1}^{5}[6!/((6-i)!i!)]=31$ different parameter groups among $2^6=64$ possible parameter assignments. These 31 parameter groups correspond to the following combinations of parameters: five entries as a linear function of one of the parameters, e.g., $[p_1]$ (among these entries, one is set as $[p_1]$ and the rest are functions of $[p_1]$) and one entry as the other parameter, e.g., $[p_2]$; four entries as a function of $[p_1]$ and two entries as a function of $[p_2]$; and three entries as a function of $[p_1]$ and three entries as a function of $[p_2]$. That is, a total of $6+15+10=31$ combinations form the parameter groups. The method of calculating the number of parameter groups using two interval parameters is applicable to any interval linear system with interval coefficient matrix and interval right-hand side vector.

For a numerical example, matrix $[\mathbf{J}] = \begin{pmatrix} [-0.745,-0.721] & [-0.487,-0.478] \\ [0.541,0.584] & [0.112,0.146] \end{pmatrix}$ and vector $[\mathbf{V}]$ of the example in Sec. 4.1 are considered. Entries $[J_{11}]$ and $[J_{12}]$ are selected as interval parameters $p_1\in[-0.745,-0.721]$ and $p_2\in[-0.487,-0.478]$, entry $[J_{21}]$ is assigned as a function of $[p_1]$, entry $[J_{22}]$ as a function of $[p_2]$, and v_x and v_y are real. Applying Eqs. (13)–(16), the two-parameter solution set is formulated as follows:

$$\dot{\boldsymbol{\theta}}(p_1,p_2) = \begin{pmatrix} \dfrac{2.714[p_2]+1.922}{1.922[p_1]-1.844[p_2]+1.965[p_1][p_2]} \\ \dfrac{-0.749[p_2]-1.844}{1.922[p_1]-1.844[p_2]+1.965[p_1][p_2]} \end{pmatrix} \tag{19}$$

The boundary lines of the solution set for each group of parametric linear system are specified by four lines; two lines $\dot{\boldsymbol{\theta}}(p_1,\underline{p}_2)$ and $\dot{\boldsymbol{\theta}}(p_1,\overline{p}_2)$ in two-dimensional space when p_1 varies from $\underline{p}_1$ to $\overline{p}_1$ and p_2 is set to the lower bound and upper bound, respectively. Similarly, the other two lines $\dot{\boldsymbol{\theta}}(p_2,\underline{p}_1)$ and $\dot{\boldsymbol{\theta}}(p_2,\overline{p}_1)$ are formulated when p_2 varies from $\underline{p}_2$ to $\overline{p}_2$ and p_1 is set to the lower bound and the upper bound, respectively. In the resulting enclosed solution set with four lines, each line is attached to the other two lines in two end points and the two attached lines share a point. Therefore, four points $\dot{\boldsymbol{\theta}}(\underline{p}_1,\underline{p}_2)$, $\dot{\boldsymbol{\theta}}(\overline{p}_1,\overline{p}_2)$, $\dot{\boldsymbol{\theta}}(\underline{p}_1,\overline{p}_2)$, and $\dot{\boldsymbol{\theta}}(\overline{p}_1,\underline{p}_2)$ form the vertices of the solution set for each parameter group. The two-parameter solution set in Eq. (19) is illustrated in Fig. 2(*b*). This solution set, solid lines, lies inside the exact solution, dashed lines.

To characterize the exact solution, first all parameter groups which result in different solution sets are determined and then plotted in $\dot{\theta}_1-\dot{\theta}_2$ plane. In this example, since there are four interval entries in the Jacobian matrix, there exist $(1/2)\sum_{j=1}^{3}[4!/((4-j)!j!)]=7$ different parameter groups. The combinations of $[\mathbf{J}]$ including two entries as functions of $[p_1]$ and two entries as functions of $[p_2]$, which lead to different solution sets, are derived and categorized as parameter groups. These three-parameter groups are $\begin{pmatrix} [p_1] & [J_{12}([p_2])] \\ [p_2] & [J_{22}([p_1])] \end{pmatrix}$, $\begin{pmatrix} [p_1] & [J_{12}([p_1])] \\ [p_2] & [J_{22}([p_2])] \end{pmatrix}$, and $\begin{pmatrix} [p_1] & [p_2] \\ [J_{21}([p_1])] & [J_{22}([p_2])] \end{pmatrix}$. The combinations of $[\mathbf{J}]$ including one entry as a function of $[p_1]$ (or $[p_2]$) and three entries as functions of $[p_2]$ (or $[p_1]$) give the remaining four parameter groups, which are $\begin{pmatrix} [p_1] & [J_{12}([p_2])] \\ [p_2] & [J_{22}([p_2])] \end{pmatrix}$, $\begin{pmatrix} [J_{11}([p_2])] & [p_1] \\ [p_2] & [J_{22}([p_2])] \end{pmatrix}$, $\begin{pmatrix} [p_2] & [J_{12}([p_2])] \\ [p_1] & [J_{22}([p_2])] \end{pmatrix}$, and $\begin{pmatrix} [J_{11}([p_2])] & [p_2] \\ [J_{21}([p_2])] & [p_1] \end{pmatrix}$. The two-parameter solution set for each parameter group is formulated similar to Eq. (19). All solution sets are illustrated with solid lines in Fig. 2(*c*), with a total of 28 lines, four lines for each parameter group. The lines connecting the outer vertices correspond to the boundary of the solution sets of $\mathbf{J}\dot{\boldsymbol{\theta}} = \mathbf{V}$, $\mathbf{J}\in[\mathbf{J}]$, which are represented with dashed lines in Figs. 2(*a*)–2(*d*).

When the exact solution is concave, the two-parameter solution sets will not distinguish the indented vertices. It should be noted that the solution set for each parameter group passes through points $\dot{\boldsymbol{\theta}}(\underline{p}_1,\overline{p}_2)$ and $\dot{\boldsymbol{\theta}}(\overline{p}_1,\underline{p}_2)$ which are the start and end points of one-parameter solution set. These points are two vertices of the solution sets for all parameter groups.

4.3 Three-Parameter Solution Set. In the three-parameter case, i.e., $K=3$, the interval entries of the coefficient matrix and right-hand side vector are linearly formulated in terms of $[p_1]$, $[p_2]$, or $[p_3]$. In this case, each parameter group includes interval parameters $[p_1]$, $[p_2]$, and $[p_3]$, and at least three interval entries in the Jacobian matrix and twist are required. The procedure to calculate the solution set for each parameter group is similar to that of the two-parameter case. Unlike $K=2$, in the case of $K=3$, there is no explicit equation in terms of the total number of entries of the Jacobian matrix and the twist, η, to formulate the number of parametric groups. In a three-parameter case, $K=3$, the number of parametric groups in any coefficient matrix $[\mathbf{J}]\in\mathbb{R}^{2\times2}$ with four interval entries, $\eta=4$, and real twist is six and listed as $\begin{pmatrix} [J_{11}([p_1])] & [p_2] \\ [p_1] & [p_3] \end{pmatrix}$, $\begin{pmatrix} [J_{11}([p_1])] & [p_1] \\ [p_2] & [p_3] \end{pmatrix}$, $\begin{pmatrix} [J_{11}([p_1])] & [p_2] \\ [p_3] & [p_1] \end{pmatrix}$, $\begin{pmatrix} [p_2] & [p_1] \\ [J_{21}([p_1])] & [p_3] \end{pmatrix}$, $\begin{pmatrix} [p_2] & [p_3] \\ [J_{21}([p_1])] & [p_1] \end{pmatrix}$, and $\begin{pmatrix} [p_2] & [p_1] \\ [p_3] & [J_{22}([p_1])] \end{pmatrix}$. If all entries of the Jacobian matrix and twist are interval, $\eta=6$, there will be 90 different parameter groups among $3^6=729$ possible parameter assignments. These parameter groups are calculated in the following manner: four entries as a linear function of one of the parameters, e.g., $[p_1]$, one entry as a linear function of parameter $[p_2]$, and one entry as a linear function of parameter $[p_3]$; three entries as a function of $[p_1]$, two entries as a function of $[p_2]$, and one entry as a function of parameter $[p_3]$; and two entries as a function of $[p_1]$, two entries as a function of $[p_2]$, and two entries as a function of $[p_3]$. Therefore, a total of $15+60+15=90$ combinations constitute the parameter groups.

For the three-parameter case, the solution set corresponding to each parameter group consists of 12 lines; the two parameters p_1, p_2 are set to either lower or upper bounds and the resulting four lines, which are functions of parameter p_3, are plotted when p_3 varies within the lower and upper bounds. The process is repeated when $[p_1], [p_3]$ are set to either lower or upper bounds and the next four lines are functions of $[p_2]$. The last four lines are formulated as functions of $[p_1]$ when $[p_2], [p_3]$ are set to either the lower or upper bounds. The boundary of the exact solution is formed by the collection of lines of different parameter groups. For example, four lines of the corresponding solution set in Fig. 2(*d*) contribute to the boundary of the exact solution. Similar to the two-parameter case, the solution set for each parameter group passes through the start and end points of one-parameter solution set.

To show the solution set for one group of parametric linear system, the same example as the two-parameter case is considered. For entries $[J_{11}]$, $[J_{12}]$, and $[J_{21}]$ as interval parameters $p_1 \in [-0.745, -0.721]$, $p_2 \in [-0.487, -0.478]$, and $p_3 \in [0.541, 0.584]$, respectively, $[J_{22}]$ is taken as a function of $[p_1]$, and v_x and v_y are real values. This three-parameter solution set is plotted in Fig. 2(*d*). As illustrated, some edges of this solution set lie on the boundary of the exact solution. The boundary of the exact solution is identified considering the solutions for all groups of parametric linear systems and selecting the outer edges. In Fig. 2(*d*), the outer enclosures form the exact solution.

4.4 Jacobian Matrix With Inconsistent Entries.

In addition to the case with two translational motions of the end effector, the case when the motion is characterized as one translation and one rotation is outlined. The Jacobian matrix that relates the joint velocity vector $\dot{\boldsymbol{\theta}} = [\dot{\theta}_1 \dot{\theta}_2]^{\mathrm{T}}$ to the end effector twist $\mathbf{V} = [v_x\ \omega_z]^{\mathrm{T}}$ in the 2DOF planar serial manipulator of Fig. 1, with equal link lengths of 0.5 m without uncertainty, is calculated as

$$\mathbf{J} = \begin{bmatrix} -0.5\sin(\theta_1+\theta_2) - 0.5\sin(\theta_1) & -0.5\sin(\theta_1+\theta_2) \\ 1 & 1 \end{bmatrix} \tag{20}$$

The manipulator is constrained to be planar, and hence, the axes of the two revolute joints are parallel and the entries of the second row in the Jacobian matrix are real numbers. For the desired twist of $\mathbf{V} = [v_x\ \omega_z]^{\mathrm{T}} = [1\ \ 1]^{\mathrm{T}}$, the vector of the joint velocity is calculated as

$$\dot{\boldsymbol{\theta}} = \mathbf{J}^{-1}\mathbf{V} = \begin{pmatrix} \dot{\theta}_1 \\ \dot{\theta}_2 \end{pmatrix} = \begin{pmatrix} \dfrac{2-\sin([\theta_1]) - \sin([\theta_1]+[\theta_2])}{4} \\ \dfrac{2-\sin([\theta_1]+[\theta_2])}{4} \end{pmatrix} \tag{21}$$

For the joint variables $\theta_1 = (\pi/6)$ (rad) and $\theta_2 = (\pi/4)$ (rad) and the radius of uncertainty $(\pi/180)$ (rad) for revolute joints, $\delta\theta_1 = \delta\theta_2 = (\pi/180)$ (rad), their interval will be $[\theta_1] = [0.506, 0.541]$rad and $[\theta_2] = [0.768, 0.803]$ rad. Substituting the interval D–H parameters into the Jacobian matrix in Eq. (20) yields the interval Jacobian matrix $[\mathbf{J}] = \begin{pmatrix} [-0.745, -0.721] & [-0.487, -0.478] \\ [1,1] & [1,1] \end{pmatrix}$. Since there are two interval entries in the Jacobian matrix, $\eta = 2$, there is just $(1/2)\sum_{j=1}^{\eta-1}(\eta/j) = (1/2)\sum_{j=1}^{1}[2!/((2-j)!j!)] = 1$ parameter group $\begin{pmatrix} [p_1] & [p_2] \\ [J_{21}([p_1])] & [J_{22}([p_1])] \end{pmatrix}$ for the two-parameter case. The second row of the Jacobian matrix is not interval, and hence, coefficients $J_{21,1}$ and $J_{22,1}$ in Eq. (11) are zero and $J_{21,0} = J_{22,0} = 1$. The two-parameter solution set is illustrated in Fig. 2(*e*). The second row of $[\mathbf{J}]\dot{\boldsymbol{\theta}} = [\mathbf{V}]$ corresponds to the angular velocity of end effector $\dot{\theta}_1 + \dot{\theta}_2 = 1$. Therefore, the solution set is a line with the slope of -1. If the two revolute joints were not parallel due to uncertainty, i.e., motion out of plane were allowed, the coefficients of $J_{21,1}$ and $J_{22,1}$ would be nonzero and the solution set would be a polygon.

4.5 Exact Solution; Convex or Concave.

The exact solution is formulated using all parameter groups for the specific number of interval parameters. It is noteworthy that the one-parameter solution set is always inside the two-parameter and three-parameter solution sets. In general, for K-parameter case, the number of lines involved to form the solution set for each parameter group is $K \times 2^{(K-1)}$. For instance, in the three-parameter case, the number of lines which forms the solution set is $3 \times 2^2 = 12$. It should be noted that as the size of the interval matrix, specifically the interval entries of the matrix, increases, the total number of the parameter groups grows drastically.

The drawback of the two-parameter solution set is that the indented vertices of the exact solution, if there is any, may be ignored. The three-parameter solution set overcomes this limitation as more lines are contributed to characterize each three-parameter solution set, and the vertices of the nonconvex exact solution set are obtained. As an example, the following interval linear system is considered:

$$\begin{pmatrix} [2,3] & [0,1] \\ [1,2] & [2,3] \end{pmatrix} \begin{bmatrix} x_1 \\ x_2 \end{bmatrix} = \begin{pmatrix} [10,10] \\ [60,60] \end{pmatrix} \tag{22}$$

The solution derived by the two-parameter solution sets is depicted in Fig. 3(*a*). The black thick lines represent the boundary of the exact solution set and the dashed lines are the boundary of the two-parameter solution sets. As shown, the two-parameter solution sets cannot identify the indented vertices. In Fig. 3(*b*), the boundary of the three-parameter solution sets coincides with the boundary of the exact solution. Determining the convexity of the exact solution depends on the properties of the interval Jacobian matrix and the interval twist, and can be investigated as a future work.

5 Case Study

In this section, two example manipulators are considered.

Example 1. A 3DOF spherical manipulator with revolute–revolute–prismatic (RRP) layout (as shown in Fig. 4(*a*)) is considered. In serial manipulators with uncertainty in kinematic parameters, the interval Jacobian matrix and the end effector twist form an interval linear system, and the joint velocity vector is characterized by solving the parametric linear system. The rows of the 6×3 Jacobian matrix that correspond to the three translational motions are used in this example. For the joint displacements $\mathbf{q} = [\theta_1\ \ \theta_2\ \ d_3]^{\mathrm{T}} = [\pi/8\ \ \pi/4\ \ 1]^{\mathrm{T}}$ (rad, m), radius of uncertainty $(\pi/360)$ rad in the revolute joint displacements and 0.01 m in the prismatic joint displacement, the 3×3 interval Jacobian matrix of the manipulator will be

$$[\mathbf{J}] = \begin{pmatrix} [-0.282, -0.260] & [0.639, 0.668] & [0.645, 0.661] \\ [0.639, 0.668] & [0.260, 0.282] & [0.263, 0.279] \\ [0,0] & [-0.720, -0.694] & [0.700, 0.713] \end{pmatrix} \tag{23}$$

For the desired platform twist of $\mathbf{V} = [v_x\ v_y\ v_z]^{\mathrm{T}} = [0.5\ \ 0.1\ \ 0.3]^{\mathrm{T}}(\mathrm{m/s})$, the exact solution is calculated using the method of Sec. 4.2 for two-parameter solution set. That is, for all possible groups of two interval parameters, i.e., 255 parameter groups, the two-parameter solution sets are calculated and plotted

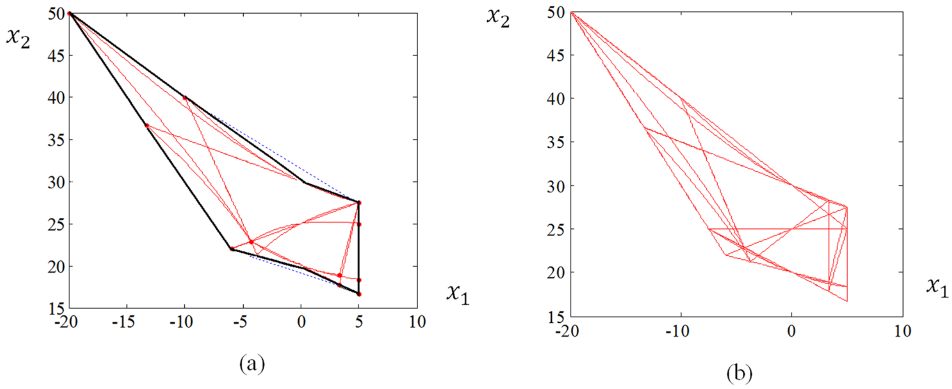

Fig. 3 (*a*) Two-parameter solution set, dotted lines, and the exact solution, solid lines, and (*b*) three-parameter solution set

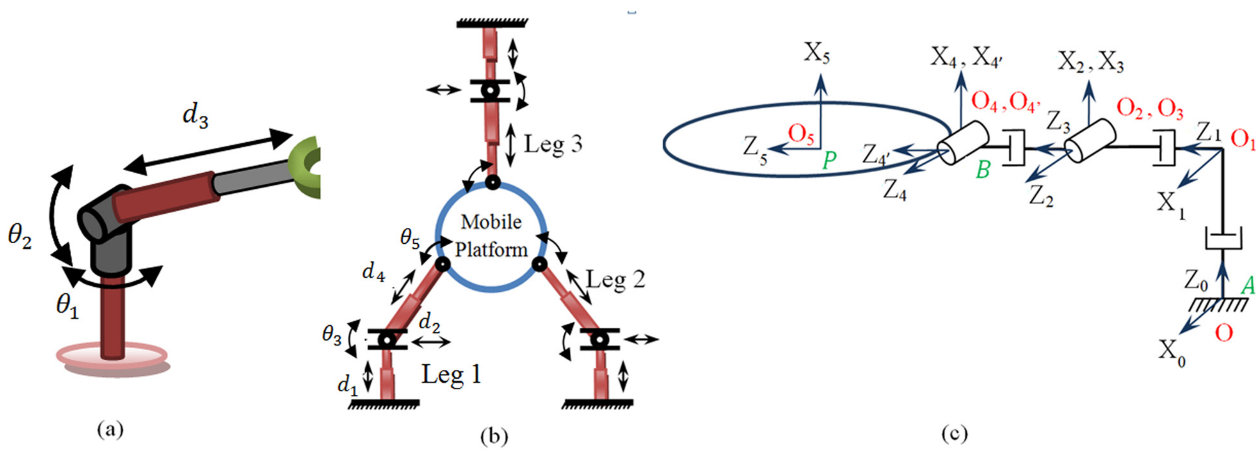

Fig. 4 (*a*) A 3DOF spherical manipulator with RRP layout, (*b*) a reconfigurable planar parallel manipulator with PPRPR layout, and (*c*) zero configuration of the legs of the parallel manipulator

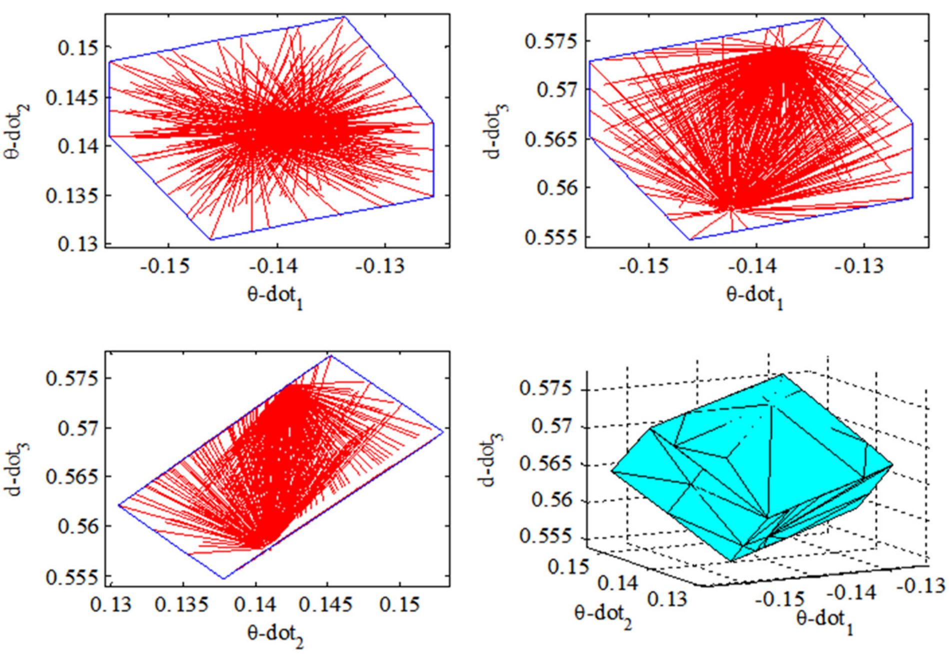

Fig. 5 Exact solution of the joints in spherical manipulator with RRP layout

Table 1 D–H parameters of the legs for parallel manipulator of Fig. 4(*b*)

From frame	θ_i (rad)	d_i (m)	a_i (m)	α_i (rad)	β_i (rad)	To frame
0	0	d_1	0	$\pi/2$	0	1
1	$\pi/2$	d_2	0	$\pi/2$	0	2
2	θ_3	0	0	$-\pi/2$	0	3
3	0	d_4	0	$\pi/2$	0	4
4	θ_5	0	0	$-\pi/2$	0	4′
4′	0	$r_{B/P}$	0	0	0	5

Table 2 Radius of uncertainty in D–H parameters for the legs of parallel manipulator of Fig. 4(*b*)

From frame	$\delta\theta_i$ (rad)	δd_i (m)	δa_i (m)	$\delta\alpha_i$ (rad)	$\delta\beta_i$ (rad)	To frame
0	0	0.01	0	$\pi/180$	0	1
1	0	0.01	0.01	0	0	2
2	$\pi/180$	0	0.01	0	0	3
3	0	0.01	0.01	0	0	4
4	$\pi/180$	0	0.01	0	0	4′
4′	0	0.01	0.01	0	0	5

(as shown in Fig. 5). Then, the outer boundary of all solution lines forms the exact solution which is shown in Fig. 5. It should be noted that the two-parameter and three-parameter methods provide the same solution as the exact solution is convex. The plot of the exact solution for all three joints (lower right plot of Fig. 5) shows that the exact solution for this manipulator is a polyhedron.

The parametric method could be easily extended to motion analysis of parallel manipulators because each leg of a parallel manipulator is a serial manipulator and the required twist of the parallel manipulator has to be in the range space of the Jacobian matrix of each leg as well as the Jacobian matrix of the parallel manipulator. The following discussions relate to a leg of the parallel manipulator of Fig. 4(*b*). The exact solution of the joint velocity vector in the interval linear system of each leg is derived considering the interval Jacobian matrix in the corresponding leg and the platform twist.

Example 2. The parallel manipulator depicted in Fig. 4(*b*) has three reconfigurable legs, each leg has five joints and two degrees of kinematic redundancy. The task space dimension of the manipulator is $m = 3$ which consists of two translations in the plane and one rotation about an axis perpendicular to the plane. Each leg has identical (prismatic-prismatic-revolute-prismatic-revolute, PPRPR) layout while only three out of five joints are used for each reconfigured case. For each case, the prismatic joints are active and revolute joints are passive. The coordinates of the base attachment points in the fixed reference frame are $(-2.000, -1.500)$m, $(2.000, -1.500)$m, and $(0.0, 1.500)$m, respectively. Leg i is attached to the base and to the platform at ${}^iA$ and ${}^iB$, respectively. The superscript i represents the number associated with the leg of the parallel manipulator. The position of connection points ${}^iB$ on the platform, $ri_{B/P}$, is set at a constant radius of 0.25 m. The manipulator center of mass is point P and the angular coordinates of the leg connections to the platform are -150 deg, -30 deg, and 90 deg, respectively.

To model the manipulator, the pose of the platform relative to the base reference frame is specified using the D–H convention. When the two consecutive joint axes are not near parallel, four independent variables are sufficient to represent the pose of the two adjacent coordinate frames. For near-parallel joint axes, the fifth parameter, rotation about the y-axis, is added to the existing four parameters. The D–H parameters corresponding to the zero configuration of the legs of the manipulator of Fig. 4(*b*) are the same and listed in Table 1.

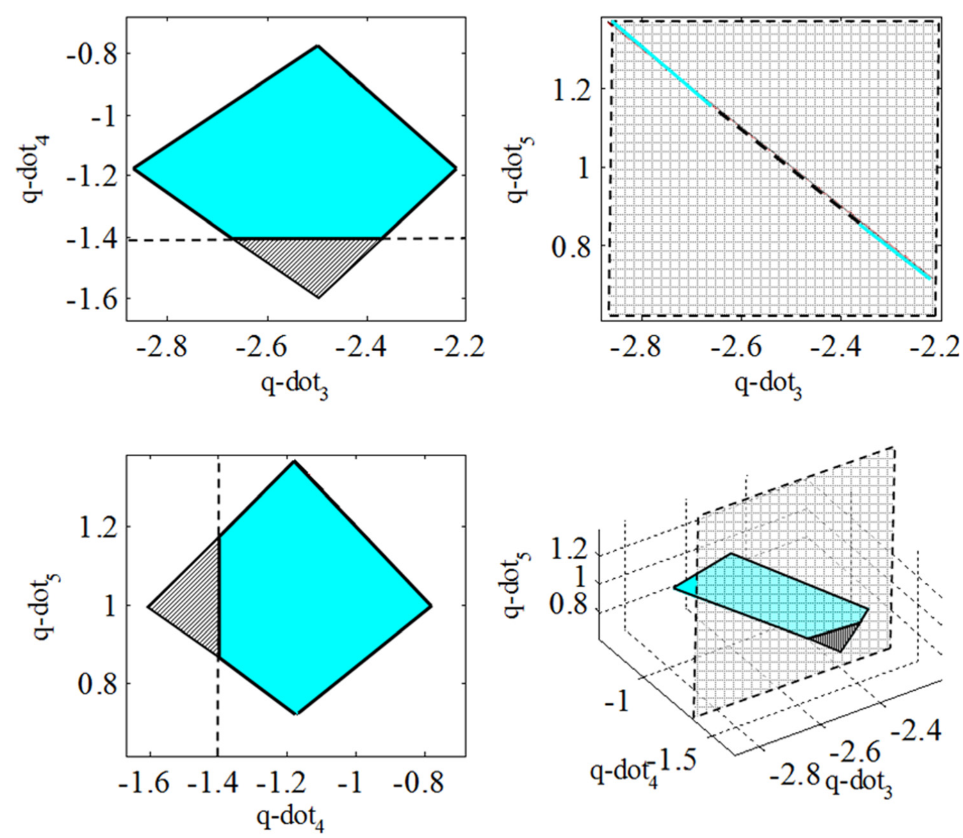

Fig. 6 Exact solution, hatched and filled areas; and feasible solution, filled area, for the joints of leg 3 of parallel manipulator of Fig. 4(*b*) with the first and second prismatic joints locked

Since the approach direction of the platform, Z_5, is normal to the axis of the last joint, Z_4, a dummy frame with origin at the origin of frame $X_4Y_4Z_4$ and orientation of frame $X_5Y_5Z_5$ is required in order to include the link parameter $r_{B/P}$ between frames $X_4Y_4Z_4$ and $X_5Y_5Z_5$ using D–H convention. The uncertainties of D–H parameters are listed in Table 2. To avoid spatial movement in each leg, the uncertainties are assigned so that the motion of the manipulator is restricted in the plane. The uncertainty in each parameter is given by an interval using midpoint-radius representation, i.e., the midpoint of the intervals is the nominal value of the parameter listed in Table 1 and the corresponding radius of uncertainties is reported in Table 2. For instance, the uncertainty in displacement of the first prismatic joint in leg 3 is given by the interval $[{}^3d_1 - {}^3\delta d_1, {}^3d_1 + {}^3\delta d_1]$.

In this example, the first and second prismatic joints of leg 3 in the parallel manipulator are locked; however, these joints have uncertain displacements in their joint axes. In other words, these joints can have any displacements in the range within ${}^3[d_1] = [-0.01, 0.01]$m and ${}^3[d_2] = [0.115, 0.135]$m. For the joint displacements ${}^3\mathbf{q} = [\,{}^3\theta_3 \quad {}^3d_4 \quad {}^3\theta_5\,]^{\mathrm{T}} = [\,-\pi/4 \quad 1.283 \quad \pi/3\,]^{\mathrm{T}}$ (m, rad) and uncertainties as reported in Table 2, the interval Jacobian matrix is

$$[{}^3\mathbf{J}] = \begin{pmatrix} [-0.932,-0.753] & [-0.732,-0.682] & [0.029,0.101] \\ [-1.239,-1.060] & [0.682,0.732] & [-0.2778,-0.206] \\ [1,1] & [0,0] & [1,1] \end{pmatrix} \tag{24}$$

The desired platform twist is $\mathbf{V} = [\mathrm{v}_x v_y \omega_z]^{\mathrm{T}} = [\,3.000 \quad 1.800 \quad -1.500\,]^{\mathrm{T}}$ (m/s, rad/s). The lower and upper limits of joint four actuator (third prismatic joint) are taken as ${}^3\dot{q}_{\min} = -1.400\,\mathrm{m/s}$ and ${}^3\dot{q}_{\max} = 1.400\,\mathrm{m/s}$. The exact solution for leg 3 of parallel manipulator is illustrated in Fig. 6. The exact solution is generated using two-parameter solution set explained in Sec. 4.2. The shape of the exact solution is an inclined plane with the slope of -1 in ${}^3\dot{q}_3 - {}^3\dot{q}_5$ plane (plane ${}^3\dot{q}_3 - {}^3\dot{q}_5$ corresponds to the velocities of the two revolute joints), the plot in the upper right-hand corner in Fig. 6. Because the two revolute joints are parallel, the third equation of the interval linear system using the Jacobian matrix in Eq. (24) is ${}^3\dot{q}_3 - {}^3\dot{q}_5 = -1.5$. Hence, the exact solution is a plane (two-dimensional). If the two revolute joints were not parallel due to uncertainty, the coefficients of ${}^3\dot{q}_3 - {}^3\dot{q}_5$ in the third equation in Eq. (24) would be interval and the solution set in ${}^3\dot{q}_3 - {}^3\dot{q}_5$ plane would be a polygon. This solution is depicted in Fig. 6, filled area. The dashed lines on the left-hand side plots correspond to the vertical grid plane depicted in the right-hand side plots and represent the boundary of the velocity limit of joint 4. For this example, the calculated portion of solution that lies within the joint limits is depicted in the filled area. The interval calculation in this paper is performed using INTLAB [25].

6 Conclusions

The goal of this paper was to characterize the solution set for the interval linear system with square coefficient matrices. The proposed method was based on parameterizing the interval entries of the coefficient matrix and right-hand side vector. The number of parametric groups was determined for two- and three-parameter cases. The two-parameter case was employed to calculate the exact solution of the interval linear system using the vertices of the solution sets corresponding to the parameter groups. In the three-parameter case, the edges of the solution sets of the parameter groups formed the boundary of the exact solution. In the interval linear systems with higher dimensions, the shape of the solution set could be quite complicated. The parametric method could be implemented to these systems as the mathematical complexity of the proposed method does not depend on the system dimension.

The parametric method was implemented for the motion analysis of 2DOF and 3DOF planar and spatial manipulators. Interval arithmetic was applied to include the uncertainty of kinematic parameters in the model of manipulators. The size and shape of the solution set depended on several factors such as the link lengths, the joint displacements, the range of uncertainties, the layout of the manipulator, the required twist, and the pose of the end effector.

References

[1] Roth, Z., Mooring, B., and Ravani, B., 1987, "An Overview of Robot Calibration," IEEE J. Rob. Autom., **3**(5), pp. 377–385.
[2] Dawood, H., 2011, *Theories of Interval Arithmetic: Mathematical Foundations and Applications*, Lambert Academic Publishing, Saarbrücken, Germany.
[3] Moore, R. E., 1966, *Interval Analysis*, Prentice Hall, Englewood Cliffs, NJ.
[4] Rao, R. S., Asaithambi, A., and Agrawal, S. K., 1998, "Inverse Kinematic Solution of Robot Manipulators Using Interval Analysis," ASME J. Mech. Des., **120**(1), pp. 147–150.
[5] Merlet, J., 2004, "Solving the Forward Kinematics of a Gough-Type Parallel Manipulator With Interval Analysis," Int. J. Rob. Res., **23**(3), pp. 221–235.
[6] Merlet, J. P., and Daney, D., 2001, "A Formal-Numerical Approach to Determine the Presence of Singularity Within the Workspace of a Parallel Robot," 2nd Workshop on Computational Kinematics, Seoul, South Korea, May 20–22, pp. 167–176.
[7] Tagawa, K., Takami, H., Shiraki, K., and Haneda, H., 2001, "Optimal Configuration Problem of Redundant Arms Considering Endpoint Compliance and Its Solution Using Interval Analysis," Trans. Soc. Instrum. Control Eng., **37**(10), pp. 990–992.
[8] Carreras, C., and Walker, I. D., 2001, "Interval Methods for Fault-Tree Analysis in Robotics," IEEE Trans. Reliab., **50**(1), pp. 3–11.
[9] Daney, D., Nicolas, A., Gilles, Ch., and Yves, P., 2006, "Interval Method for Calibration of Parallel Robots: Vision-Based Experiments," Mech. Mach. Theory, **41**(8), pp. 929–944.
[10] Oettli, W., 1965, "On the Solution Set of a Linear System With Inaccurate Coefficients," J. Soc. Ind. Appl. Math., Ser. B, **2**(1), pp. 115–118.
[11] Hansen, E., and Smith, R., 1967, "Interval Arithmetic in Matrix Computations, Part II," SIAM J. Numer. Anal., **4**(1), pp. 1–9.
[12] Neumaier, A., 2008, *Interval Methods for Systems of Equations*, Cambridge University Press, Cambridge, UK.
[13] Oettli, W., Prager, W., and Wilkinson, J., 1965, "Admissible Solutions of Linear Systems With Not Sharply Defined Coefficients," J. Soc. Ind. Appl. Math., Ser. B, **2**(2), pp. 291–299.
[14] Hartfiel, D., 1980, "Concerning the Solution Set of $Ax = B$ Where $P \leq A \leq Q$ and $P \leq B \leq Q$," J. Numer. Math., **35**(3), pp. 355–359.
[15] Hansen, E., 1992, "Bounding the Solution of Interval Linear Equations," SIAM J. Numer. Anal., **29**(5), pp. 1493–1503.
[16] Jansson, C., 1991, "Interval Linear Systems With Symmetric Matrices, Skew-Symmetric Matrices and Dependencies in the Right Hand Side," J. Comput., **46**(3), pp. 265–274.
[17] Rump, S. M., 1994, "Verification Methods for Dense and Sparse Systems of Equations," *Topics in Validated Computations, Studies in Computational Mathematics*, J. Herzberger, ed., Elsevier, Amsterdam, pp. 63–136.
[18] Popova, E., and Krämer, W., 2008, "Visualizing Parametric Solution Sets," BIT Numer. Math., **48**(1), pp. 95–115.
[19] Moore, R. E., Cloud, M. J., and Kearfott, R. B., 2009, *Introduction to Interval Analysis*, SIAM, Philadelphia.
[20] Paul, R. P., 1981, *Robot Manipulators: Mathematics, Programming, and Control: The Computer Control of Robot Manipulators*, MIT Press, Cambridge, MA.
[21] Hayati, S. A., 1983, "Robot Arm Geometric Link Parameter Estimation," 22nd IEEE Conference on Decision and Control (CDC), San Antonio, TX, Dec. 14–16, Vol. 22, pp. 1477–1483.
[22] Rohn, J., 2005, "A Handbook of Results on Interval Linear Problems," http://www.Cs.Cas.Cz/Rohn/Handbook
[23] Popova, E. D., 2004, "Strong Regularity of Parametric Interval Matrices," 33rd Spring Conference of the Union of Bulgarian Mathematicians: Mathematics and Education in Mathematics, Borovetz, Bulgaria, Apr. 1–4, pp. 446–451.
[24] Hladík, M., 2012, "Enclosures for the Solution Set of Parametric Interval Linear Systems," Int. J. Appl. Math. Comput. Sci., **22**(3), pp. 561–574.
[25] Rump, S. M., 1999, "INTLAB—INTerval LABoratory," *Developments in Reliable Computing*, T. Csendes, ed., Kluwer Academic Publishers, Dordrecht, The Netherlands, pp. 77–104.